DOI: 10.1002/JLB.5MA0420-375RRRRR

JLB JOURNAL OF LEUKOCYTE BIOLOGY

MEETING ARTICLE

TNFR2 blockade alone or in combination with PD-1 blockade shows therapeutic efficacy in murine cancer models

Katherine Case[1] | Lisa Tran[1] | Michael Yang[1] | Hui Zheng[2] | Willem M. Kuhtreiber[1] | Denise L. Faustman[1]

[1]Immunobiology Laboratory, Massachusetts General Hospital and Harvard Medical School, Boston, Massachusetts, USA

[2]Biostatistics Center, Massachusetts General Hospital, Boston, Massachusetts, USA

Correspondence
Denise L. Faustman, Massachusetts General Hospital and Harvard Medical School, Building 149, 13th Street, Room 3602, Boston, MA 02129, USA.
Email: Faustman@helix.mgh.harvard.edu

Abstract

Immune checkpoint inhibitors are profoundly transforming cancer therapy, but response rates vary widely. The efficacy of checkpoint inhibitors, such as anti-programmed death receptor-1 (anti-PD-1), might be increased by combination therapies. TNFR2 has emerged as a new target due to its massive expression on highly immunosuppressive regulatory T cells (Tregs) in the microenvironment and on certain tumor cells. In murine colon cancer models CT26 and MC38, we evaluated the efficacy of a new anti-TNFR2 antibody alone or in combination with anti-PD-1 therapy. Tumor-bearing mice were treated with placebo, anti-PD-1 alone, anti-TNFR2 alone, or combination anti-PD-1 and anti-TNFR2. We found that combination therapy had the greatest efficacy by complete tumor regression and elimination (cure) in 65–70% of animals. The next most effective therapy was anti-TNFR2 alone (20–50% cured), whereas the least effective was anti-PD-1 alone (10–25% cured). The mode of action, according to in vivo and in vitro methods including FACS analysis, was by killing immunosuppressive Tregs in the tumor microenvironment and increasing the ratio of CD8+ T effectors (Teffs) to Tregs. We also found that sequence of antibody delivery altered outcome. The two most effective sequences were simultaneous delivery (70% cured) followed by anti-TNFR2 preceding anti-PD-1 (40% cured), and the least effective was by anti-PD-1 preceding anti-TNFR2 (10% cured). We conclude that anti-PD-1 is best enhanced by simultaneous administration with anti-TNFR2, and anti-TNFR2 alone may be potentially useful strategy for those do not respond to, or cannot tolerate, anti-PD-1 or other checkpoint inhibitors.

KEYWORDS

ADCC, antibodies, cancer, checkpoint blockade, combination immunotherapy, immunotherapy, oncology, PD-1, Teff, TNFR2, Tregs

1 | INTRODUCTION

Immunotherapy has strikingly improved cancer survival with the use of blocking antibodies to programmed death receptor-1 (PD-1) or programmed death-ligand 1 (PD-L1), among others, but response rates differ, depending on cancer type.[1-4] New immunotherapies are needed to combine with checkpoint inhibitors to boost their efficacy, or to use as alternative single agents. One targeted approach presented here is designed to shift the tumor microenvironment toward tumor cell death by depletion of suppressive regulatory T cells (Tregs), which, in turn, lifts suppression of tumor-specific T effectors (Teffs). The purpose is to reinvigorate so-called "exhausted" tumor-specific Teffs to enhance their cytotoxic function against the tumor.

The TNFR2 receptor sets the balance between Tregs and Teffs (also known as cytotoxic T cells); the receptor acts as a bidirectional switch that can cause Treg cell expansion (with agonism) or Treg contraction (with antagonism).[6,7] TNFR2-expressing Tregs or myeloid suppressor cells in the tumor infiltrate are the most potent immunosuppressive cells identified to date that dampen the host immune response.[8,9] TNFR2 agonism is potentially therapeutic in diverse human autoimmune diseases where there are too many Teffs and too few highly expressing TNFR2-expressing Treg cells.[10] By contrast, TNFR2 antagonism is potentially therapeutic in many cancers where there are too many TNFR2-expressing Tregs in the tumor microenvironment and too few Teffs, often referred to as exhausted T cells. The

Abbreviations: ADCC, antibody-dependent cellular cytotoxicity; PD-1, programmed death receptor-1; Teff, T-effector cells; Tregs, regulatory T cells.

Received: 6 September 2019 | Revised: 1 April 2020 | Accepted: 14 April 2020

accumulation of TNFR2-expressing Tregs in the tumor microenvironment or soluble TNFR2 in the serum carry poor prognosis in human and mice tumors.[11-14] In the CT26 colon cancer model and the 4T1 breast mouse model, antibodies that block TNFR2 signaling enhance survival alone or in combination with other therapies such as CpG and anti-CD25 antibodies.[15] Murine testing of TNFR2 combined with PD-1 antagonistic antibodies has not yet been reported.

TNFR2 is an attractive target for cancer immunotherapy[16] TNFR2 in the human is an identified oncogene across diverse cancer types.[17,18] The exact genetic mutations of TNFR2 itself or the signaling pathway it involves are not fully identified in every cancer type. We are defining oncogene as mutations in the case of human lymphomas and human myelofibrosis and on tumor tissue as the aberrant expression on a parenchymal cell or cell line when the normal cells do not express this protein linked to a well-known growth pathway. TNFR2 overexpression is also observed on myeloid-derived monocyte suppressor cells, another target in the tumor microenvironment.[19] Human data suggests that after checkpoint failures in metastatic melanoma, TNFR2 can be even more highly expressed in the tumor microenvironment on Tregs, acting as a possible escape mechanism after failed therapy.[20] Our previously identified human-directed TNFR2 antagonistic antibodies in culture kill tumor-infiltrating Tregs, proliferate tumor associated Teffs, and also directly kill human oncogene expressing tumor cells, but with lessened activity against normal lymphoid cells outside the tumor microenvironment.[21,22] Human-directed TNFR2 antagonistic antibodies can directly kill Tregs with the natural agonistic ligand TNF present and do not require antibody-dependent cellular cytotoxicity (ADCC) or Fc receptor function, a feature that likely will improve their toxicology profile, as will TNFR2's limited body-wide expression.[21] Likewise human-directed TNFR2 antagonistic antibodies have specificity for only rapidly proliferating Tregs in the tumor microenvironment with little or lessened activity against nontumor associated circulating human Tregs.[21,22]

Here we identify and begin to characterize a new murine-directed TNFR2 antibody (TY101; hereinafter referred to as anti-TNFR2) that possesses features of previously identified human-directed TNFR2 antagonistic antibodies. We evaluate its therapeutic activity alone or in combination with anti-PD-1 antibody in vitro and in vivo in two mouse models of colon cancer, CT26 and MC38. We also test the mode of action by evaluating the impact on Tregs and Teffs in tumor cell infiltrates using FACS analysis. Finally, we evaluate the best sequence of delivery of both antibody therapies to optimize combination immunotherapy.

2 | MATERIALS AND METHODS

2.1 | Protein gel electrophoresis

Monoclonal antibody protein samples were run on NativePAGE 4–16% Bis-Tris gel with Tris-Glycine Native Running Buffer (Life Technologies, Carlsbad, CA, USA) at 225 V for 2.5 h. Gels were stained for 30 min with Pierce Silver Stain (Thermo Fisher Scientific, Inc., Waltham, MA, USA) under nonreducing conditions according to the manufacturer's instructions. Antibody protein samples were also run on NuPAGE 4–12% Tris/glycine gels with NuPAGE LDS sample buffer (Life Technologies), NuPAGE sample reducing agent (Life Technologies), and Tris/glycine/SDS running buffer (Life Technologies) at 200 V for 35 min. Gels were stained for 45 min with SimplyBlue SafeStain (Invitrogen, Carlsbad, CA, USA) under reducing conditions.

2.2 | Strong cation exchange (SCX) fractionation with HPLC

SCX fractionation was performed on an Agilent 1260 model HPLC. Key components included Quat Pump model number: G1311B, Multiwavelength detector model number: G1365C, Fraction Collector model number G1330B. Data analysis was performed on Agilent Chemstation. The column used was a Proteomix SCXNP5 4.6 × 250 mm column from Sepax Technologies, Inc. (Newark, Delaware, USA; catalogue number 401NP5-4625PK). Running conditions were as follows: flow rate: 1 mL/min, detector: UV 280 nm, column temperature: 25°C. A total of 20 μL of the antibody was directly injected on to the column in each run. The sample was kept at 4°C in a temperature controlled autosampler. The mobile phase was composed of 2-Morpholinoethanesulfonic acid„ 4-Morpholinepropanesulfonic acid, TRIS-hydroxymethyl methylamino propanesulfonic acid, 3-cyclohexyl-2-hydroxy-1-propanesulfonic acid, NaCl, and Milli Q water. Each run had a gradient of mobile phase A of 5% mobile and this was compared to phase B of 35% mobile during a 30 min period followed by 2 min of isocratic flow. A 4.5 min wash in mobile phase C was performed at the end of each gradient to clean the column. Fractions were collected and subsequently pooled. Purity of each fraction was verified by HPLC run on the same column and same instrument. The recovery yield was calculated by comparing peak area between the crude and purified sample after normalizing for injection volume and concentration. Pooled fractions were stored at 4°C.

2.3 | Impact on Treg cells with TNFR2 antagonistic antibodies

CD4+ cells were isolated using the EasySep Mouse T cell Isolation Kit (catalogue #19852) from normal nontumor-bearing mice. Isolated CD4+ cells were re-suspended in RPMI 1640; GlutaMAX (Life Technologies) plus 10% FBS (Sigma-Aldrich, St louis, MO), murine IL2 (100 U/ml) (Sigma-Aldrich), and 1% penicillin streptomycin (Life Technologies). Cells were seeded at a concentration of 0.2×10^6 cells per well in 96-well round-bottom plates, treated with the TNFR2 antagonist, and incubated at 37°C and 5% CO2 for 72 h. After incubation, cells were collected by centrifugation, washed once with 1× HBSS (Invitrogen, Carlsbad, CA, USA), and stained for FACS analysis. FACS data were processed using FlowJo software (version 10.1).

2.4 | Reagents and flow cytometry

Cells were prepared for flow cytometry using mouse regulatory T cell staining kit #2 (catalogue #88-8118-40, Thermo Fisher Scientific, Inc., Waltham, MA, USA) according to the manufacturer's instructions. Fluorescently stained cells were resuspended in 1× HBSS

(Invitrogen, Carlsbad, CA, USA) and analyzed using a BD FACS Calibur Flow Cytometer machine (Becton Dickinson, Franklin Lakes, NJ, USA). Antibodies used for FACS analysis of Tregs included clone FJK-165 anti-mouse FOXP3 for intracellular staining of FOXP3 and clone PC61.5 anti-mouse CD25 (Thermo Fisher Scientific, Inc., Waltham, MA, USA). Treg populations and Teff/Treg ratios were assessed by FACS. Antibodies for in vivo studies were anti-mouse PD-1 (CD279, clone RMP-14) (BioXCell, West Lebanon, NH, USA) and the anti-mouse TNFR2 (TY101), which was isolated from a collection of antibodies within the Harvard and MGH Antibody Cores (Boston, MA, USA). This collection of research reagents were internally produced antibodies donated from various investigators and screened by our group for the desired activities. After confirming the intended immunogen was TNFR2 or a fragment of TNFR2, the initial screening on murine TNFR2 ELISA plates for TNFR2 binding was initiated. These screens also included early confirmation of no TNFR1 binding. If sole TNFR2 binding was observed, all new antibodies to mouse TNFR2 continued into functional assays. Immunoprecipitation gels showed that the protein brought down by TY101 was mouse TNFR2 by the use of polyclonal anti-TNFR2 immunoblotting methods.

For functional assays, the Treg cells within isolated mouse CD4 cells were demonstrated to be killed after brief 48–72 h timing on murine splenocytes in a dose-specific manner. Longer incubation times at the start were performed to confirm cell disappearance and also flow cytometry experiments included a total cell count. The moderate duration of the incubation time was chosen so an antibody dose response could be observed. We selected the best antibody with these traits. Because in humans we were knowledgeable of the optimized TNFR2 receptor binding sites for dominant antagonism, defined as antagonism that is not disrupted by the natural ligand TNF, we next characterized the mouse-directed lead candidate with TNF in the media to confirm it remained an antagonist and the used the Pepscan technology using the precision epitope mapping methods (Pepscan, Lelystad, The Netherlands). Antibody TY101 was the lead candidate based on binding to only mouse CRD3 and CRD4 TNFR2 receptor regions, similar to our past screening of human-directed antagonistic antibodies. This receptor site binding is believed to result in the formation of TNFR2 anti-parallel dimers that block the TNF binding site.[15,20] This is the near identical binding region for the optimized human antibodies, only reactive to the human TNFR2 receptor with strong antagonism. TY101 was then moved forward into additional characterization studies outlined in the paper. TY101 was purified using affinity chromatography followed by PBS solution. The purity of the antibody was >95%. Bacterial endotoxin levels were determined using the Endosafe-PTS system and Endosafe PTS cartridges (Charles River Laboratories, Wilmington, MA). Antibody concentration was determined by measuring absorbance at 280 nm and the results were calculated using the standard extinction coefficient 205, 500 M^{-1} cm^{-1} for 1.0 mg/ml = A280.

2.5 | Isolation of tumor infiltrating lymphocytes

Tumors were surgically dissected from mice and then dissociated using Miltenyi Dissociation kit protocol (catalogue #130-096-730) (Miltenyi Biotec, Inc., Somerville, MA, USA). After dissociation, 2 mL/sample of 1× lysing buffer was used to further lyse any contaminating RBCs. Cell were incubated for 20 min on a tube rocker at room temperature. Cells were centrifuged at 300× *g* for 4°C for 5 min. After the centrifugation 2 mL of FACS Buffer was added to the cells and centrifuged at 300× *g* for 4°C for 5 min. Cells were re-suspended in 0.5–1 mL FACS buffer and were counted and used for FACS staining.

2.6 | In vitro killing assays of murine tumor cells treated with TNFR2 antagonistic antibodies

CT26 and MC38 cells were purchased from ATCC and grown up in medium of RPMI GlutaMAX (Life Technologies) plus 10% FBS (Sigma-Aldrich, St louis, MO), IL2 (100 U/ml) (Sigma-Aldrich, St louis, MO), and 1% penicillin streptomycin. CT26 and MC38 cells were cultured in 96-well round-bottom plates at a concentration of 1×10^4 cells per well in 200 µl of media. Cells were treated directly with TNFR2 antagonistic antibodies and incubated for 7 d. This time period was chosen after optimization experiments were first conducted. The goal was to confirm under extended incubation conditions such as 14 d, the cells were totally eliminated. We then chose a more moderate incubation time to monitor dose responses of a test antibody. After incubation, cells were detached from the plate and stained with trypan blue (Sigma-Aldrich, St louis, MO) to count viable cells.

2.7 | In vivo efficacy analysis

Mice were tested and monitored for tumor growth by either Champions Oncology (Hackensack, NJ, USA) or an independent third party. Animals were randomized to receive subcutaneous injection into the flank with two different mouse tumor cell lines (CT26 and MC38). Animals were dosed with antibody once tumors reached a volume between 100 and 200 mm^3. Animals were dosed biweekly i.p. with 100 µg twice per week anti-PD-1 or/and anti-TNFR2 antibody. Unless otherwise specified all antibodies administered in vivo had endotoxin <1 EU/mg. Tumor volumes were measured manually with calipers by blinded examiner over a 20 or 21 d course. Animals were euthanized if tumor sizes reached 1500 mm^3 or the tumor ulcerated through the skin. The flow gating methods for the tumor into single cell suspensions and then gating on select populations is shown in Supporting Information Figure S1.

2.8 | Pepscan mapping studies

The 3D peptide mapping of anti-TNFR2 binding to TNFR2 was performed using chemically linked peptides on scaffolds (CLIPS) technology (Pepscan). Briefly, the target protein was converted into a library of up to 10,000 overlapping linear peptides, which were then bound to a solid support and shaped into a matrix of CLIPS constructs. The affinity of the antibody to the various peptide conformations were used to determine the precise discontinuous epitopes.

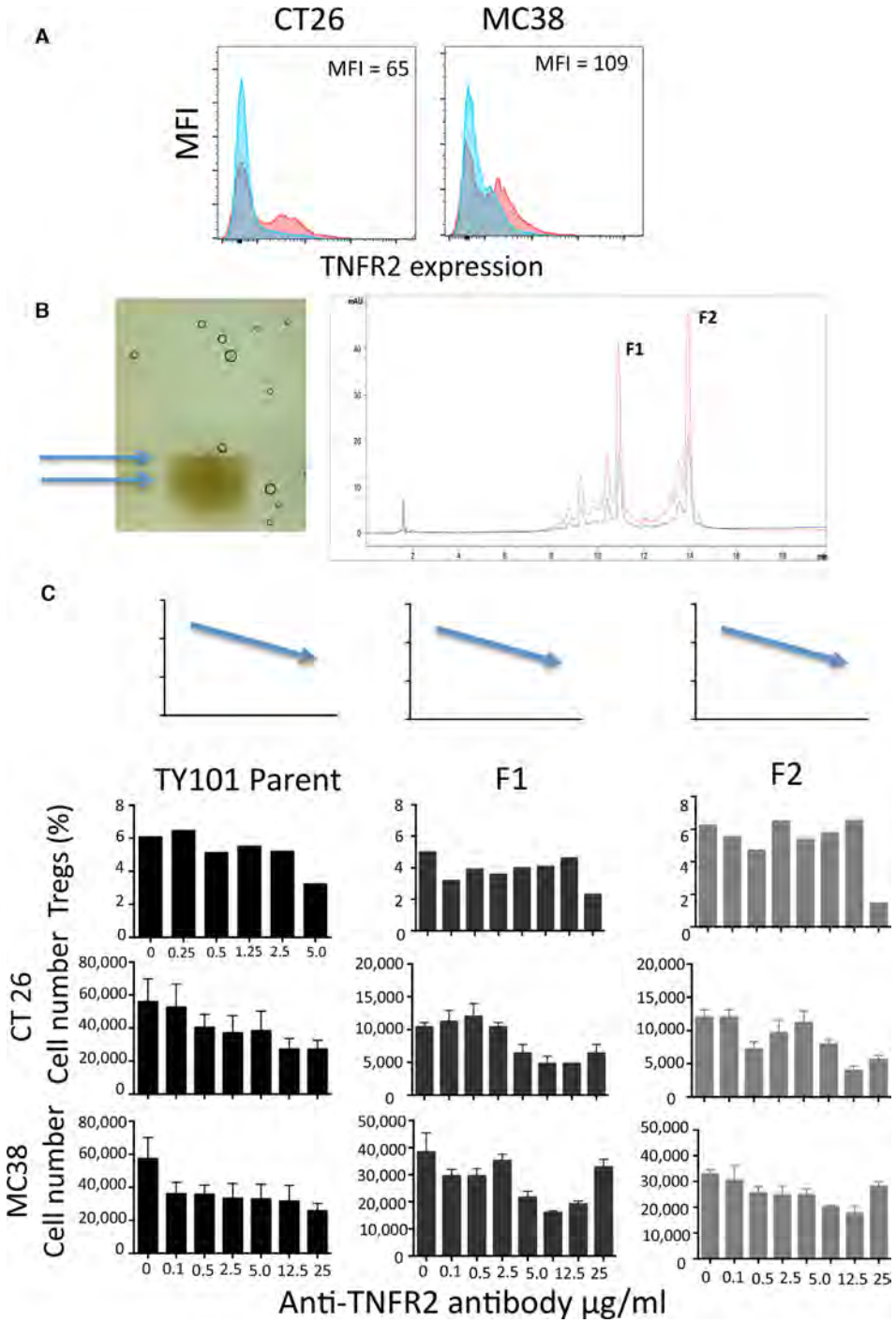

FIGURE 1 **Murine-directed TNFR2 antagonistic antibody exhibits mild in vitro cytotoxic activity against regulatory T cells (Tregs) and tumor cell lines.** (**A**) Low expression of TNFR2 on murine colon cancer cell lines. The mean fluorescent intensity (MFI) of TNFR2 was measured on mouse colon cancer cell lines CT26 (left) and MC38 (right). CT26 tumor cells showed lower expression of the aberrantly expressed TNFR2 protein (MFI = 65); MC38 tumor cells also had low expression but slightly higher than CT26 (MFI = 109). Pink represents TNFR2 staining; blue is background staining with an isotype control. This is a representative experiment but the experiment performed >10 times. (**B**) A nonreducing gel of the mouse-directed IgG1 TNFR2 antagonist (TY101) showed two distinct bands (left). These isoforms were separated by HPLC (right) into two fractions (F1 and F2). (**C**) The parent anti-TNFR2 antibody (TY101) and its two HPLC separated band fractions (F1 and F2) were tested for cytotoxic function against three potential targets: Tregs (CD4+ cells) from normal mice and TNFR2-low expressing tumor cells (CT26 and MC38). Freshly isolated CD4+ cells were treated with the parent antibody, HPLC fraction F1, and fraction F2 (0 to 25 µg/mL) for 72 h, whereas CT26 and MC38 tumor cells were treated for 7 d. The dose–response for the parent TNFR2 antagonist (TY101) (column 1) as well as each fraction (columns 2 and 3), showed mild Treg, MC38, and CT26 cell killing. Data are expressed as mean ± SEM for at least $n = 6–7$ experiments/group for the MC38 and CT26 killing. For the splenic Treg killing by the three antibody fractions, a characteristic Treg experiment was presented (the experiment was performed two times). The mixed effects statistical model showed for both TY101 and fraction F1 and F2 a downward slope. All killing slopes against the tumor cell lines showed a change from baseline that was statistically significant ($P < 0.05$)

2.9 | Statistical analysis

Data analysis was performed by Student's *t*-test using Excel (Microsoft) or GraphPad Prism 5 software (GraphPad Software). Significance was determined by $P < 0.05$.

3 | RESULTS

3.1 | CT26 and MC38 cell lines express low levels of TNFR2, making them susceptible to modest anti-TNFR2-induced cell death in vitro

We profiled CT26 and MC38 murine tumor cells for aberrant TNFR2 surface expression using flow cytometry. Figure 1A shows that both CT26 and MC38 tumor cells had low yet stable aberrant TNFR2 expression. Using nonreducing SDS gels we next observed that the mouse-directed IgG1 TNFR2 antibody (TY101) expressed two antibody bands (Fig. 1B, left). The bands were separable by HPLC and had identical sequences. Multiple antibody bands on nonreducing gels are often due to the amino acid sequences of the hinge region forming different disulfide linkages. On reducing gels, anti-TNFR2 showed only one heavy chain and one light chain, confirming the suspected interchain disulfide hinge variations previously described (Supporting Information Fig. S2).

Next we examined the functional capacity in vitro of the parent antibody (anti-TNFR2 antibody, TY101) and each of the two HPLC isolated antibody fractions, F1 and F2 (Fig. 1B, right, Fig. 1C). The desired trend line is downward Treg cells as the dose of antibody is increased, even when tested on nontumor microenvironment CD4 T cells isolated from normal mice (Fig. 1C, top row). Anti-TNFR2 antibody displayed modest killing of normal mouse CD4 Tregs cells in a dose–response manner (Fig. 1C, second row, left most panel). The CD4 Tregs were isolated from normal spleen, because of insufficient numbers of T-lymphocytes to harvest from the tumor microenvironment. The tumor microenvironment shows more pronounced Treg killing with TNFR2 antagonistic antibodies but in mice this experiment is not feasible due to small tumor volumes; therefore, normal splenocytes were used for screening antibodies. The tumor microenvironment shows more pronounced Treg kills of TNFR2 antagonistic antibodies but in mice this experiment is not feasible. Furthermore, both F1 and F2 HPLC-separated antibody fractions retained this modest dose–response killing of murine Tregs (Fig. 1C, top row, two right-most panels). Characteristic flow cytometry histograms are represented in Supporting Information Figure S3. Similarly, anti-TNFR2 antibody modestly killed CT26 or MC38 mouse tumor cells within 7 d of exposure, and again this activity was observed in the both the F1 and F2 fractions (Fig. 1C, two bottom rows). It is important to keep in mind that, in the human, optimized antagonistic antibodies preferentially bind only newly synthesized TNFR2 proteins on rapidly proliferating tumor-infiltrating Tregs because a new inhibitory dimeric surface structure is formed or stabilized. Therefore we were not too surprised that in vitro this new antibody might not be very potent, so in vivo experiments were required scientifically.

Enzymatic removal of the Fc region of this antibody did not affect in vitro killing of Tregs or of TNFR2-expressing CT26 or MC38 cells (data not shown); therefore, this antibody did not require ADCC mechanism for activity. Detailed peptide mapping studies of the anti-TNFR2 binding region with Pepscan mapping technology confirmed binding to the CRD3 and CRD4 regions of the mouse TNFR2 receptor. These binding regions are conducive to antagonistic activity.[21]

3.2 | Anti-TNFR2 therapy alone or in combination with anti-PD-1 is efficacious in vivo in CT26-tumor implanted animals

To profile the efficacy of each antibody therapy in vivo, immunocompetent mice were first subcutaneously implanted into the flank with CT26 colorectal murine tumor cells. When tumors reached a threshold volume of 100–200 mm^3, we administered four different therapies at doses of 100 μg of sterile antibody twice per week for 20–21 d: placebo control, anti-PD-1 alone, anti-TNFR2 alone, and combination anti-PD-1+anti-TNFR2 (Fig. 2A, right). We assessed the daily impact on tumor volume by group (Fig. 2A, left), by individual animals in spider plots (Fig. 2B), by percentage of animals achieving cure (cure rate) as measured by complete tumor regression (Fig. 2C), and, in the few animals who failed to be cured, the percentage of Tregs remaining (Fig. 2D, left panel) and the ratio of CD8+ cells/Tregs in the tumor infiltrate (Fig. 2D, right panel), measured by FACS analysis.

Mice receiving the three active therapies displayed significantly smaller tumor volumes than controls ($n = 8$) (Fig. 2A). The display of the individual tumor implanted mice in Figure 2B helped to define differences between the treated mice. Anti-TNFR2 antibody ($n = 18$) was the best solo therapy based on cure rate at days 20–21 of 10/18 mice, or 55% (Fig. 2B, C). Anti-PD-1 antibody ($n = 8$) performed relatively poorly, with a cure rate of only 25% (Fig. 2B, C). Combination therapy with anti-TNFR2 and anti-PD-1 ($n = 8$) performed better than any solo therapy, with a cure rate of 62% (Fig. 2B, C).

The few surviving mice with visible but greatly reduced residual tumors at days 20–21 ($n = 2$ per study group) were studied for constituents of the tumor microenvironment, specifically the number of Tregs and the ratio of Teffs:Tregs. FACS analysis of the tumor infiltrate revealed that mice receiving either anti-TNFR2 alone or combination therapy had Treg depletion and corresponding increases in the ratio of Teffs to Tregs (Fig. 2D; Supporting Information Fig. S1). Mice treated with anti-PD-1 alone had no changes in Tregs or Teffs relative to controls as would be expected.

3.3 | Anti-TNFR2 therapy alone or in combination with anti-PD-1 is the most efficacious in vivo in MC38-tumor implanted animals as it relates to cures

MC38 tumor implanted mice receiving each of the active therapies had smaller tumor volumes than controls (Fig. 3A, left). Anti-PD-1 alone resulted in only 10% of mice being cured but still with reduced tumor volumes compared to controls ($P = 0.0002$; Fig. 3B, top right; Fig. 3C). Anti-TNFR2 alone cured 20% of the mice and again all mice had

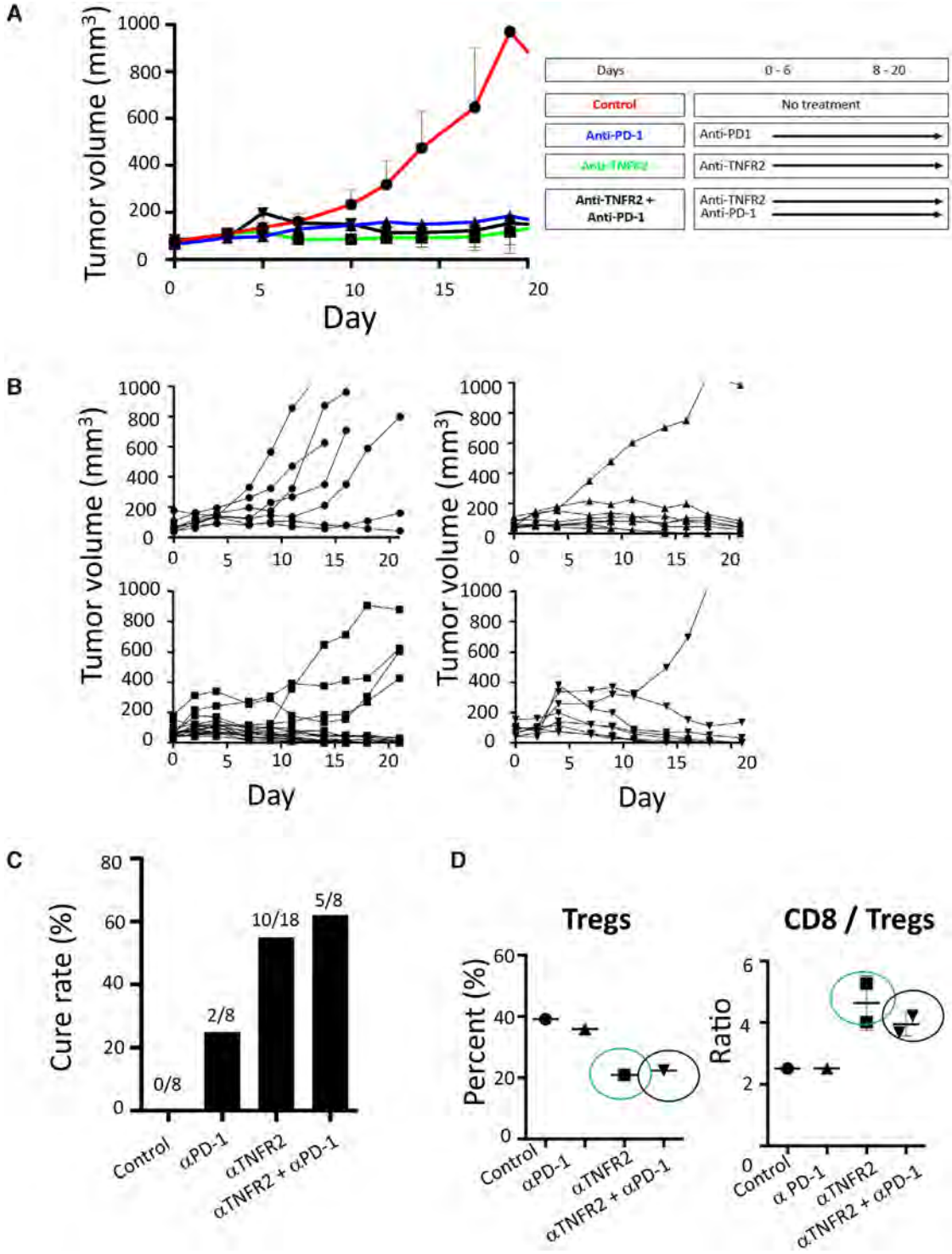

FIGURE 2 **Single and combination therapy reduced tumor volume in CT26-implanted animals.** (**A**) Schematic of therapy administration (right) with biweekly dosing with 100 μg/mouse antibody or placebo over a 20–21 d course. All three active therapy groups demonstrated a significant reduction in mean tumor volume relative to the control group. Anti-programmed death receptor-1 (anti-PD-1; 156 ± 118.72 mm^3, $P = 0.002$, $n = 8$); anti-TNFR2 (146 ± 65.95 mm^3, $P < 0.0001$, $n = 18$); and combination anti-PD-1+anti-TNFR2 (147 ± 124.33 mm^3; $P = 0.0004$, $n = 8$) tumors were all smaller than controls (798 ± 493.026 mm^3; $n = 8$). **(B)** Tumor volumes in individual animals over time using spider plots (control in top left; anti-PD-1in top right; anti-TNFR2 in bottom left; and combination therapy in bottom right). **(C)** Cure rates (complete tumor elimination) at days 20–21 were best for combination therapy (62% of animals cured) and anti-TNFR2 therapy (55% cured) and worst for programmed death receptor-1 (PD-1; 25% cured) and control (0% cured) (**D**) Flow cytometry of tumor infiltrate in the only animals with visible but shrunken tumors at day 21 showed depletion of regulatory T cells (Tregs; CD4+ T cells) and increased ratio of Teffs (CD8+ T cells) to Tregs only for anti-TNFR2 alone and combination therapy, but not for anti-PD-1 alone. Data are expressed as mean ± SEM. All statistics are the treatment group compared to the control group. Using the CT26 murine model this experiment was performed at two separate times with similar data

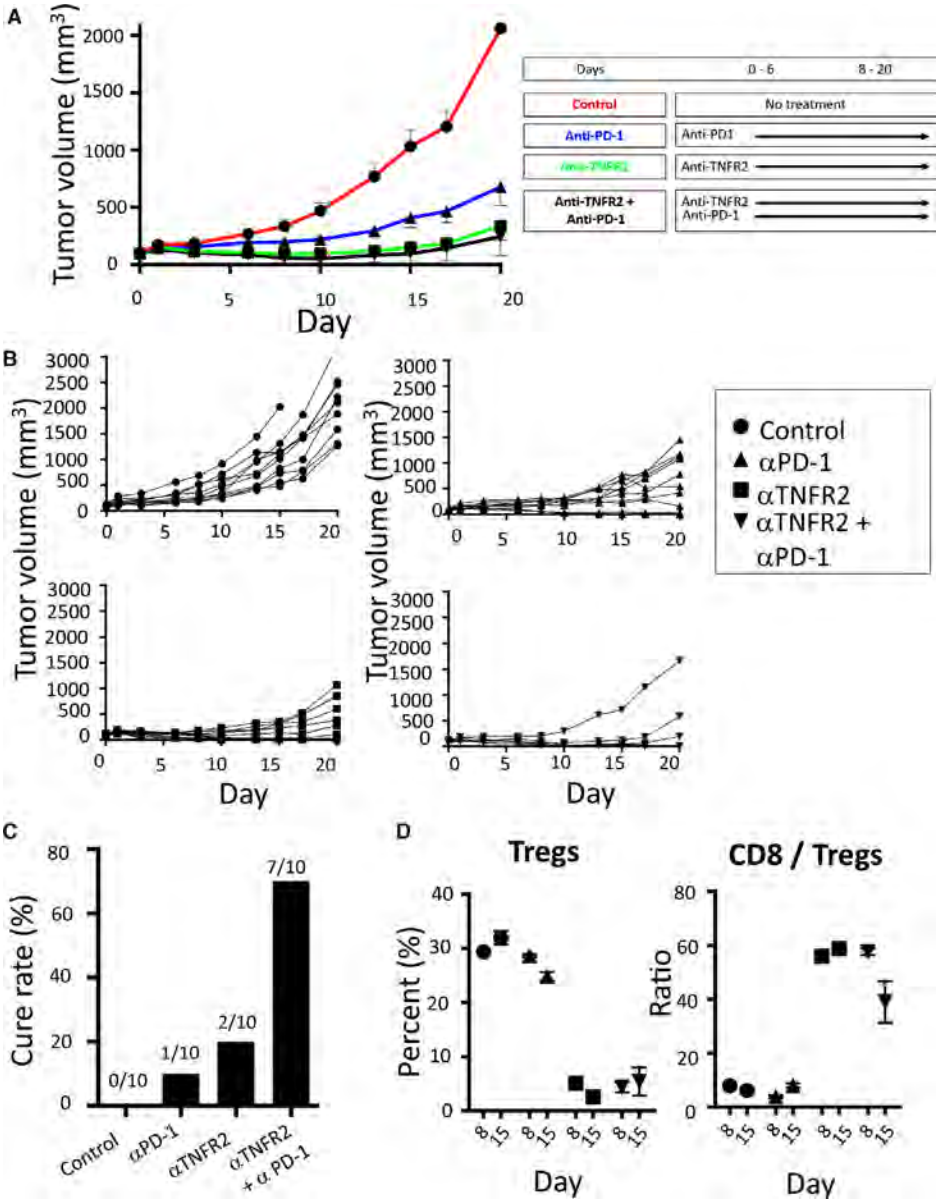

FIGURE 3 **Single and combination anti-programmed death receptor-1 (anti-PD-1) and anti-TNFR2 therapy reduce tumor volume in MC38-implanted mice.** (**A**) Schematic of therapy administration, right panel, in which mice were dosed biweekly with 0.1 mg/kg of anti-PD-1, anti-TNFR2, or combination anti-TNFR2 + anti-PD-1 therapy, and mean tumor volumes were measured over a 20–21 d course (left panel). All three active treatment groups demonstrated a significant reduction in tumor growth relative to control. Anti-TNFR2 alone and the combination anti-TNFR2+anti-PD-1 therapy showed greater improvement (vs. control) than did anti-PD-1 alone (left). Control group (2064 ± 210.15 mm^3; $n = 10$), anti-PD-1 (680 ± 165.00 mm^3; $P = 0.0002$, $n = 10$), anti-TNFR2 (336 ± 122.94 mm^3; $P < 0.0001$, $n = 10$), and combination therapy (245 ± 168.71 mm^3; $P < 0.0001$, $n = 10$) (**B**) Individual tumor volumes are shown (control in top left; anti-PD-1in top right; anti-TNFR2 in bottom left; and combination therapy in bottom right). (**C**) Cure rates (complete tumor elimination) at days 20–21 were best for combination therapy (70% of animals cured) and anti-TNFR2 therapy (20% cured) and worst for programmed death receptor-1 (PD-1; 10% cured) and control (0% cured). (**D**) Flow cytometry of tumor infiltrate at day 8 ($n = 8$) and day 15 ($n = 8$) were performed for each treatment condition to capture the evolution of tumor infiltrates and prevent bias at days 20–21, a time point where only failed animals could be samples. Anti-TNFR2 and anti-TNFR2 therapy with anti-PD1 were the therapies to most dramatically to deplete regulatory T cells (Tregs; CD4+ T cells) ($P = 0.0142$, $P = 0.0179$) and increase CD8+/Treg ratio ($P = 0.0044$, $P = 0.0072$) at day 15. Data are expressed as mean ± SEM. Using the MC38 murine model this experiment was performed at two separate times with similar data

significantly reduced tumor volumes ($P < 0.0001$; Fig. 2B, lower left; Fig. 3C). The combination of anti-PD-1 and anti-TNFR2 was highly efficacious, with 70% cured ($P < 0.0001$; Fig. 3B lower right; Fig. 3C). A time course of flow cytometry was performed to understand the evolution of the Tregs and CD8/Treg tumor cellular changes. The flow cytometry gating patterns are shown in Supplementary Figure S1. This was important to perform because sampling only at days 20–21, the experimental end point, leaves only a few failure mice

and many mice with no tumors so the flow cytometry picture bias is toward nonresponding mice. Both TNFR2 therapy as a sole therapy and in combination with anti-PD1 changed the tumor microenvironment with the targeted depletion of Tregs and augmented Teffs measured as the CD8/Treg ratio both at day 8 (Treg: anti-TNFR2 alone $P = 0.0045$, anti-PD1 alone $P = 0.1716$; anti-TNFR2 plus anti-PD1 $P = 0.0046$; CD8/Treg ratio: anti-TNFR2 alone $P = 0.0046$, anti-PD1 alone $P = 0.0413$, combination therapy $P = 0.0045$) and at day 15 (Treg: sole therapy $P = 0.0142$, combination therapy = 0.0179; CD8/Treg ratio: sole therapy $P = 0.0044$, anti-TNFR2 plus anti-PD1 $P = 0.0045$) (Fig. 3D, right panel).

3.4 | The sequence of antibody therapy administration alters efficacy

Two previous reports in mice given combination antibody therapy with anti-PD1 therapy suggest that the order of antibody administration significantly affects outcomes.[23,24] The impact of therapeutic sequencing in MC38-implanted mice is depicted in Figure 4. We evaluated four different antibody administration sequences (Fig. 4A, right panel): (i) control (placebo for 20 d); (ii) anti-PD-1 for 7 d followed by anti-TNFR2 until day 20; (iii) anti-TNFR2 for 7 d followed by anti-PD-1 until day 20; and (iv) the co-administration of anti-PD-1 and anti-TNFR2 for 20 d. Although each of the three active therapies is superior to control in terms of reduced tumor volume (Fig. 4A, left panel) and cure rate (Fig. 4C), the data also clearly show that antibody ordering affects efficacy. When anti-PD-1 preceded anti-TNFR2 therapy, efficacy was weakest (Fig. 4B, upper right). Efficacy was improved when anti-TNFR2 preceded anti-PD-1 (Fig. 4A, left panel, Fig. 4B lower left, Fig. 4C). This ordering of antibodies resulted in 40% cures, ($P = 0.0001$) (Fig. 4C). The best efficacy was achieved by co-administration of anti-PD-1 and anti-TNFR2, with 70% of mice cured ($P < 0.0001$) (Fig. 4B, lower right, Fig. 4C). This high efficacy rates suggest synergy compared to the other two active treatment groups. Flow cytometry was performed at both day 8, when all mice had tumors, and also at day 20, on the few remaining animals where a tumor could be found. The flow cytometry of the tumor infiltrates was studied as it is related to the order the administered antibodies. The tumor infiltrates in the anti-PD1 then anti-TNFR2 antibody combination (with low cure rates) was compared to the anti-TNFR2 followed by anti-PD1 antibody (with high cure rates). To further define the time course an early and late time points was used to better understand the tumor infiltrate evolution (Fig. 4D). An early treatment of time point of day 8 allowed sufficient tumor material prior to a cure with all mice having tumors ($n = 8$). The data show that the combination therapy of anti-PD1 first followed by anti-TNFR2 allowed persistent high Tregs and lower Teff compared to anti-TNFR2 first followed by anti-PD1 or simultaneous treatment where the Tregs were lowered. This more successful combination, or avoidance of anti-PD1 first, shows at day 8 the Treg cells decreasing and Teff increasing compared to the reverse treatment or to controls. This same comparison at day 20 demonstrated the same trend (Fig. 4D) and shows that only one of the active treatments reduced the number of Tregs: anti-TNFR2 preceding anti-PD-1 therapy or the combo together This therapy also had the highest ratio of CD8/Tregs, but it is important to keep in mind that the flow cytometry at day 20 could only be performed on the two mice with tumor remaining; thus the flow cytometry at earlier time points is likely more reflective of the tumor microenvironment changes shown in Figure 3D. Characteristic flow cytometry pictures of the tumor cell infiltrates for a day 8 and for day 20 harvested MC 38 tumors are shown (Supporting Information Figs. S4 and S5). The tumor infiltrates were evaluated to the number of Tregs and the umber of Teffs in mice receiving different treatments.

3.5 | Lowering endotoxin contamination of therapy improves in vivo efficacy

In MC38-implanted animals ($n = 90$), less endotoxin contamination (<1 endotoxin units, EU, per mg) of each of the three active therapies was associated with lower tumor volumes than the same therapy with higher endotoxin administration (<2 EU/mg) (Supporting Information Fig. S6, left vs. right columns). As a result of this experiment we used the higher purification on all other experiments reported in this study.

4 | DISCUSSION

Our study finds that (i) anti-TNFR2 immunotherapy alone or in combination with anti-PD-1 is a powerful new therapeutic approach in a commonly used mouse models of cancer; (ii) the mode of action of anti-TNFR2 appears to be by dramatically changing the tumor microenvironment with tumor-specific Treg elimination and Teff augmentation to allow the immune system of the host to become active again; and (iii) delivering anti-TNFR2 at the same time as, or before, anti-PD-1 carries the greatest benefit. Anti-PD-1 preceding TNFR2 is to be avoided.

We were surprised by the potent in vivo efficacy of anti-TNFR2 therapy compared to its lackluster in vitro killing of Tregs, CT26, and MC38 cell lines. One explanation may be that the Tregs in the in vitro experiments were from normal spleen rather than the tumor microenvironment (because of too few T cells to harvest for analysis in mouse tumors). Normal Tregs have less TNFR2 expression and less newly made TNFR2 than that on the highly suppressive Tregs of the tumor microenvironment, suggesting insufficient antagonism to be cytotoxic. TNFR2 antagonistic antibodies do not disrupt already stabilized resting TNFR2 trimers with TNF ligand; they only stabilize or make new TNFR2 dimers on rapidly dividing cells in vivo.

Based on our findings, we believe anti-tumor efficacy of TNFR2 blockade is by selective killing of high TNFR2-expressing tumor-residing Tregs that confer maximal suppression of the “exhausted” Teffs. TNFR2 antagonism kills tumor-associated Tregs by preventing signaling through NF-kB, which is necessary for Treg survival.[5] Depleting the suppressive Tregs, in turn, allows Teff awakening. Another mechanism of efficacy may be by direct killing of tumor cells, which has been found with other tumor cell lines.[21,22] It is also known that myeloid-derived suppressor cells (MDSC) express TNFR2 and this

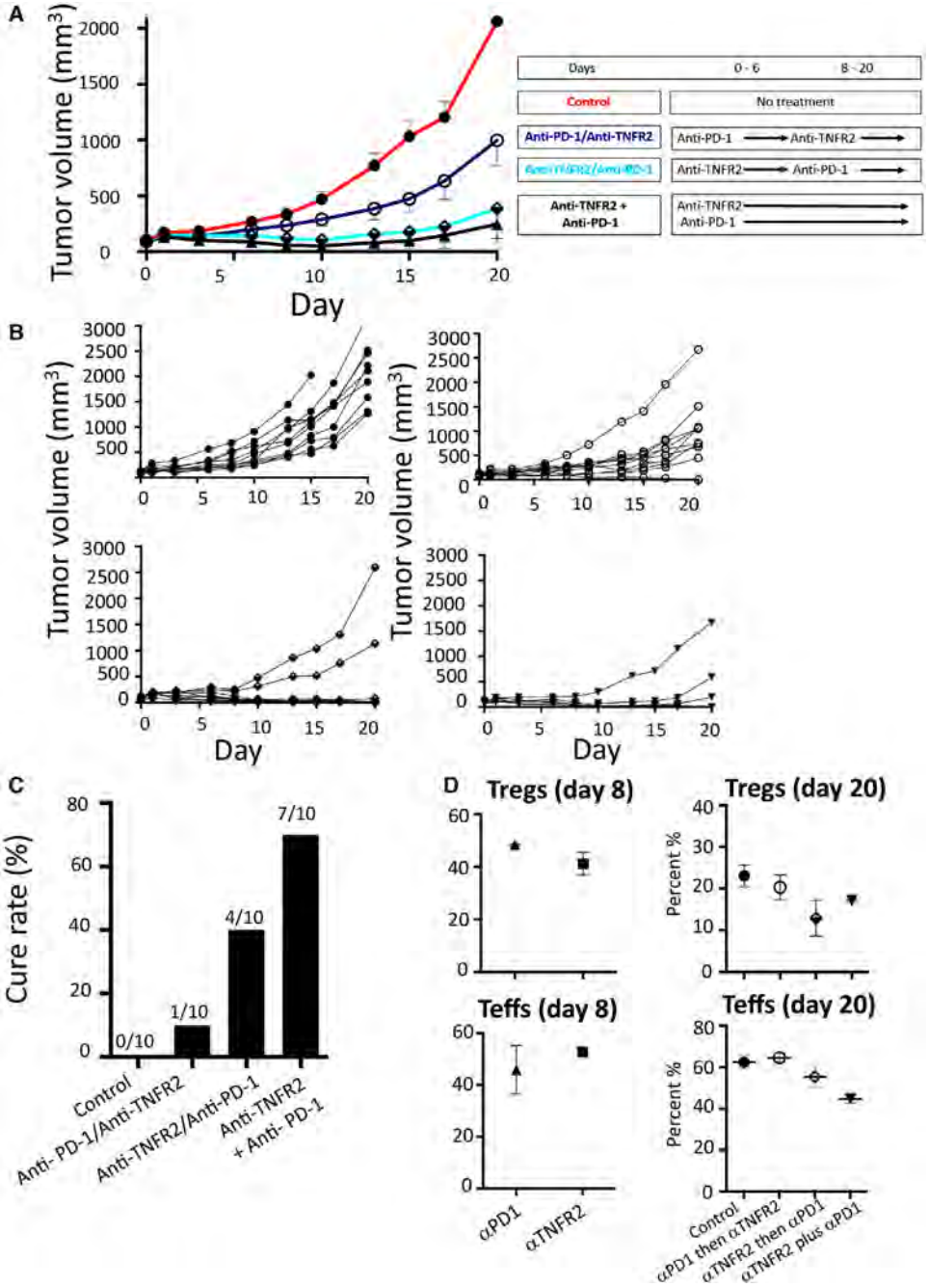

FIGURE 4 **Sequential administration of anti-programmed death receptor-1 (anti-PD-1) and anti-TNFR2 has differential effects on tumor volume in MC38-implanted mice.** (**A**) Schematic of therapy administration (Fig 4A, right). MC38-implanted mice were dosed biweekly with 0.1 mg/kg of sequential or concurrent administration of anti-PD-1 and anti-TNFR2 antibodies, and mean tumor volumes were measured over a 20–21 d course (Fig. 4A. left). Administering anti-TNFR2 before anti-PD-1 showed a significantly greater reduction in tumor volume than administering anti-PD-1 before anti-TNFR2, and this reduction was similar to the results in the simultaneous anti-TNFR2+ anti-PD-1 treatment group ($n = 10$, $n = 10$, $n = 10$). (**B**) Individual tumor volumes for control (2064 ± 210.159; $n = 10$), anti-TNFR2/ anti-PD1 (387 ± 269.563; $P = 0.0001$, $n = 10$), anti-PD1/ anti-TNFR2 (999 ±226.17; $P = 0.0003$, $n = 10$), and concurrent anti-PD1 and anti-TNFR2 treatment (245 ± 168.717; $P < 0.0001$, $n = 10$) are shown. (**C**) Cure rate (complete tumor regression) was highest for simultaneous combination therapy (70% of animals cured), followed by anti-TNFR2 first (40% cured), and last by anti-PD-1 first (10% cured) and control (0%). (**D**) Flow cytometry data of tumor infiltrate in the animals that failed to be cured revealed that anti-TNFR2 first depleted regulatory T cells (Tregs) and enhanced Teff/Treg ratio, and this effect was not observed in either the simultaneous treatment group or the group where anti-PD-1 was presented first at least for the two nonresponsive mice. Data are expressed as mean ± SEM. Using the MC38 murine model this experiment was performed one time

may also contribute to their immunosuppressive effects in the tumor microenvironment.[23]

Unlike the Tregs of the tumor environment in mice and humans, which have massive TNFR2 expression, the Teffs of the tumor microenvironment have null to suboptimal TNFR2 expression. Normal Teffs are known to have low but detectable TNFR2. PD-1 blockade is known to restore activation marker expression on Teffs to normal and to restore their proliferative abilities.[24] This may explain the significance of the sequence of delivery. We found the relatively weakest efficacy with PD-1 blockade preceding TNFR2 blockade. This sequence may inadvertently inactivate or kill the newly invigorated Teffs (in addition to the Tregs). In other words, PD-1 blockade restores TNFR2 expression to Teffs, leaving them vulnerable to inactivation or death by the TNFR2 blockade.

We are not the first group to show that combination cancer immunotherapies can often improve with selection of the proper sequencing of immunotherapy administrations. Two groups have shown that concurrent PD-1 blockade negates the effects of OX40 agonistic antibody in murine tumor models.[25,26] We now show similar but not identical data with TNFR2 antagonism; TNFR2 antagonism works best if administered first followed by PD-1 blockade or concurrently with PD-1 blockade, but loses its added efficacy if administered after PD-1 blockade. Checkpoint inhibitors nonspecifically activate the immune system and may revive the Teff response. Teff augmentation in murine models with a TNFR2 agonistic approach, especially if the tumor is deficient in Tregs, could be an alternative.[27] If pretreatment with PD-1 blockade unleashes the immune system, the benefit of a targeted immunotherapy like TNFR2 blockade is likely diminished because of greater the Teff inactivation.

This study also addresses the technical issue of endotoxin contamination of antibodies used in murine studies. Most commonly it is acceptable to use in vivo mouse antibodies with endotoxin levels of <2 EU/mg as reported broadly in the literature. What we observe here is that when mouse-directed immunotherapeutic antibodies are purified to a higher standard, such as endotoxin to levels of <1 EU/mg, the efficacy of active therapies is enhanced. This finding may be explained by endotoxin's nonspecific immune activation.

We conclude that TNFR2 blockade is a promising immunotherapy alone or, better yet, when combined with PD-1 blockade, based on results in two murine cancer models. Anti-TNFR2 alone performed better than anti-PD alone. TNFR2 blockade lacks potential for autoimmunity because only a minor subset of peripheral CD4 T cells express TNFR2, and it is likely to have a favorable toxicology profile due to its selective expression on a subpopulation of potent Tregs, myeloid suppressor cells. TNFR2 ligands, agonists, and antagonists have minimal in vivo toxicity in primates.[26] Our data also reinforce the importance of studying mechanism of action, and potency of TNFR2 antagonism alone, as well as sequence of delivery.

ACKNOWLEDGMENT

We thank Dr. Miriam Davis for the critical read and editing of the manuscript.

AUTHORSHIP

K.C., L.T., and M.Y. performed experiments; W.M.K. analyzed the results; H.Z. performed the statistics; and D.L.F. interpreted data, supervised experiments, and wrote the manuscript.

DISCLOSURES

The authors declare no conflicts of interest on the data generated in these mice experiments. Also all mouse experiments were performed by third parties blinded to the reagents to ensure data integrity and no bias.

ORCID

Denise L. Faustman https://orcid.org/0000-0002-0871-4812

REFERENCES

1. Isakov N. Immune checkpoint-targeted therapy: cancer and autoimmune diseases represent two sides of the same coin. *J Autoimmun Disord*. 2016. https://doi.org/10.21767/2471-8513.100017.
2. Zou W, Wolchok JD, Chen L. PD-L1 (B7-H1) and PD-1 pathway blockade for cancer therapy: mechanisms, response biomarkers, and combinations. *Sci Transl Med*. 2016;8:328rv4.
3. Hamanishi J, Mandai M, Matsumura N, Abiko K, Baba T, Konishi I. PD-1/PD-L1 blockade in cancer treatment: perspectives and issues. *Int J Clin Oncol*. 2016;21:462-473.
4. Darvin P, Toor SM, Sasidharan V, Elkord E. Immune checkpoint inhibitors: recent progress and potential biomarkers. *Exp Mol Med*. 2018;50:165.
5. Ban L, Zhang J, Wang L, Kuhtreiber W, Burger D, Faustman DL. Selective death of autoreactive T cells in human diabetes by TNF or TNF receptor 2 agonism. *Proc Natl Acad Sci U S A*. 2008;105:13644-13649.
6. Okubo Y, Mera T, Wang L, Faustman DL. Homogeneous expansion of human T-regulatory cells via tumor necrosis factor receptor 2. *Sci rep*. 2013;3:3153.
7. Chen X, Subleski JJ, Hamano R, Howard OM, Wiltrout RH, Oppenheim JJ. Co-expression of TNFR2 and CD25 identifies more of the functional CD4+FOXP3+ regulatory T cells in human peripheral blood. *Eur J Immunol*. 2010;40:1099-1106.
8. Tanaka A, Sakaguchi S. Regulatory T cells in cancer immunotherapy. *Cell Res*. 2017;27:109-118.
9. Govindaraj C, Scalzo-Inguanti K, Hallo MM, Flanegan K, Quinn M, Plebanski M. Impaired Th1 immunity in ovarian cancer patients is mediated by TNFR2+ Tregs within the tumor microenvironment. *Clin Immunol*. 2013;149:97-110.
10. Okubo Y, Toerrey H, Butterworth J, Zheng H, Faustman DL. Treg activation defect in type 1 diabetes; correction with TNFR2 agonism. *Clin-Transl Immunol*. 2016;5:e56. https://doi.org/10.1038/cti.2015.43.
11. Tao H, Mimura Y, Aoe K, et al. Prognostic potential of FOXP3 expression in non-small cell lung cancer cells combined with tumor-infiltrating regulatory T cells. *Lung Cancer*. 2012;75:95-101.
12. Shou J, Zhang Z, Lai Y, Chen Z, Huang J. Worse outcome in breast cancer with higher tumor-infiltrating FOXP3+ Tregs: a systematic review and meta-analysis. *BMC Cancer*. 2016. https://doi.org/10.1186/s12885-016-2732-0.
13. Lin YC, Mahalingam J, Chiang JM, et al. Activated but not resting regulatory T cells accumulated in tumor microenvironment and correlated with tumor progression in patients with colorectal cancer. *Int J Cancer*. 2013;132:1341-1350.
14. Liu L, Zhao G, Wu W, et al. Low intratumoral regulatory T cells and high peritumoral CD8(+) T cells relate to long-term survival in patients

with pancreatic ductal adenocarcinoma after pancreatectomy. *Cancer Immunol Immunother*. 2016;65:73-82.
15. Nie Y, He J, Shirota H, et al. Blockade of TNFR2 signaling enhances the immunotherapeutic effect of CpG ODN in a mouse model of colon cancer. *Sci Signal*. 2018. https://doi.org/10.1126/scisignal.aan0790.
16. Vanamee E, Faustman DL. Structural principles of tumor necrosis factor superfamily signaling. *Sci Signal*. 2018;11:eaap4910.
17. Ungewickell A, Bhaduri A, Rios E, et al. Genomic analysis of mycosis fungoides and Sezary syndrome identifies recurrent alterations in TNFR2. *Nat Genet*. 2015;47:1056-1060.
18. Cerami E. The Human Tumor Atlas Network: Data Coordinating Center. *NIH Research Portfolio Online Reporting Tools*. 2020. https://projectreporter.nih.gov/project_info_description.
19. Hu X, Li B, Li X, et al. Transmembrane TNF promotes suppressive activities of myeloid-derived suppressor cells via TNFR2. *J Immunol*. 2014;192:1320-1331.
20. Tirosh I, Izar B, Prakadan SM, et al. Dissecting the multicellular ecosystem of metastatic melanoma by single-cell RNA-seq. *Science*. 2016;352:189-196.
21. Torrey H, Butterworth J, Mera T, et al. Targeting TNFR2 with antagonistic antibodies inhibits proliferation of ovarian cancer cells and tumor-associated Tregs. *Sci Signal*. 2017. https://doi.org/10.1126/scisignal.aaf8608.eaaf8608.
22. Torrey H, Khodadoust M, Tran L, et al. Targeted killing of TNFR2-expressing tumor cells and Tregs by TNFR2 antagonistic antibodies in advanced Sézary syndrome. *Leukemia*. 2018;33:1206-1218.
23. Hu S, Li B, Li X, et al. Transmembrane TNF promotes suppressive activities of myeloid-derived suppressor cells via TNFR2. *J Immunol*. 2013;192:1320-1331.
24. Buchan S, Manzo T, Flutter B, et al. OX40- and CD27-mediated costimulation synergizes with anti-PD-L1 blockade by forcing exhausted CD8+ T cells to exit quiescence. *J Immunol*. 2015;194:125-133.
25. Shrimali RK, Ahmad S, Verma V, et al. Concurrent PD-1 blockade negates the effects of OX40 agonist antibody in combination immunotherapy through inducing T-cell apoptosis. *Cancer Immunol Res*. 2017;5:755-766.
26. Messenheimer DJ, Jensen SM, Afentoulis ME, et al. Timing of PD-1 blockade is critical to effective combination immunotherapy with anti-OX40. *Clin Cancer Res*. 2017;23:6165-6177.
27. Tam S, Fulton RB, Sampson JF, et al. Antibody mediated targeting of TNFR2 activates CD8+ T cells in mice and promotes antitumor immunity. *Sci Transl Med*. 2019;11(512):eaax0720.

SUPPORTING INFORMATION

Additional information may be found online in the Supporting Information section at the end of the article.

How to cite this article: Case K, Tran L, Yang M, Zheng H, Kuhtreiber WM, Faustman DL. TNFR2 blockade alone or in combination with PD-1 blockade shows therapeutic efficacy in murine cancer models. *J Leukoc Biol*. 2020;1–11. https://doi.org/10.1002/JLB.5MA0420-375RRRRR

Supplementary Figure 1

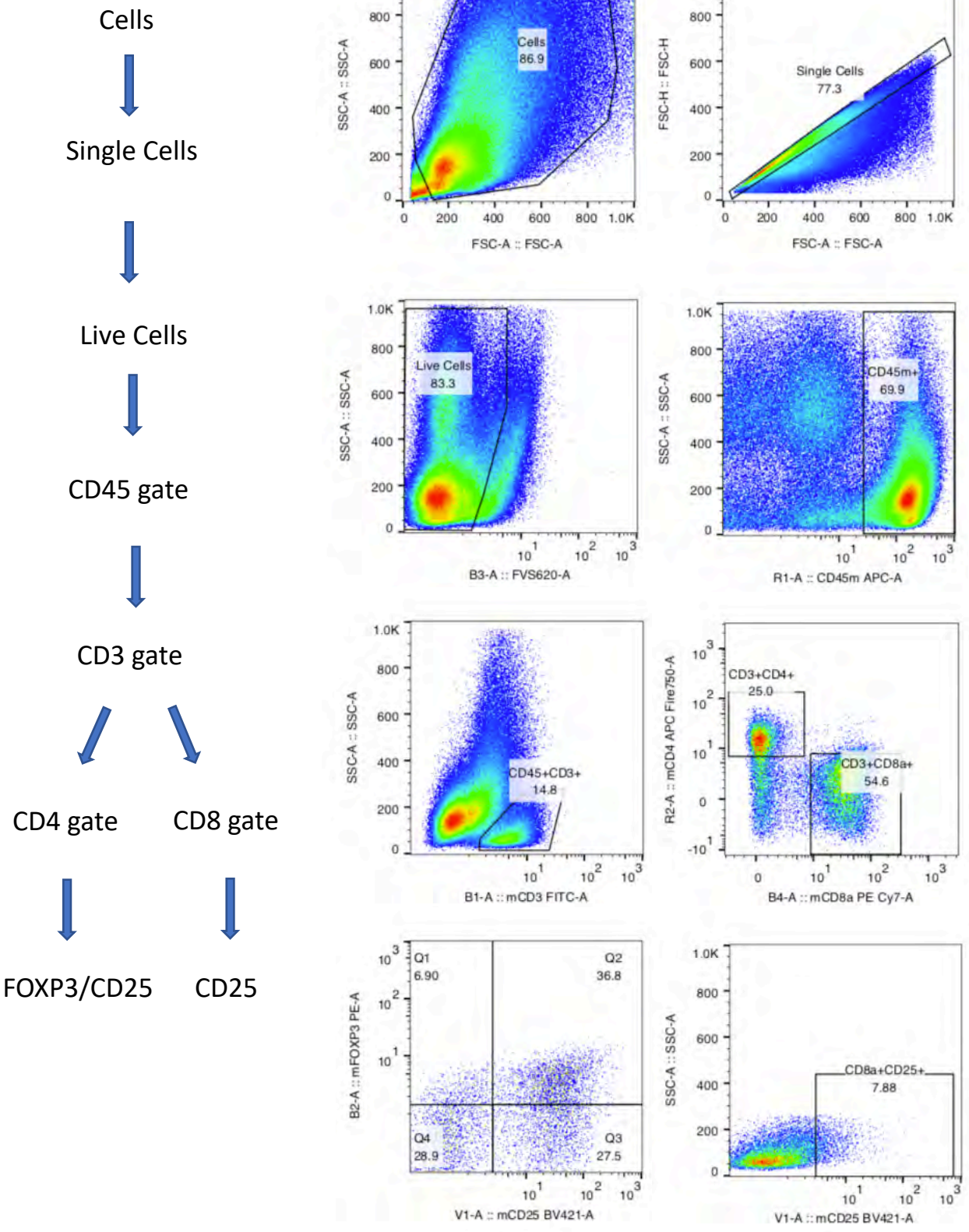

Supplementary

Figure 2

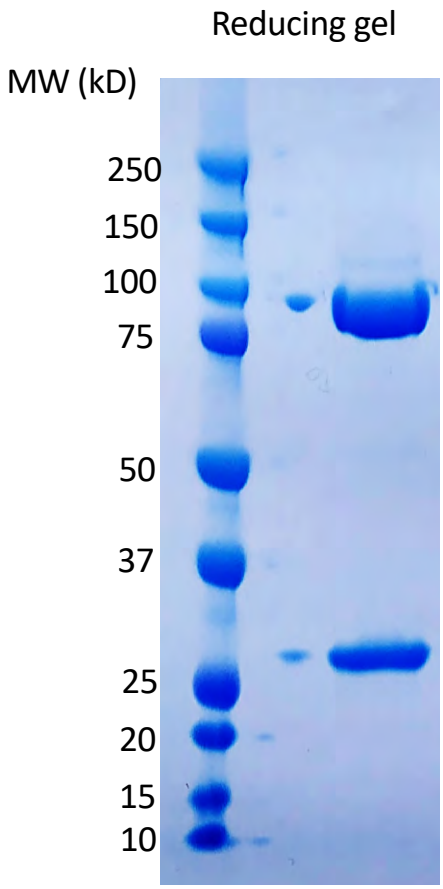

Supplementary Figure 3

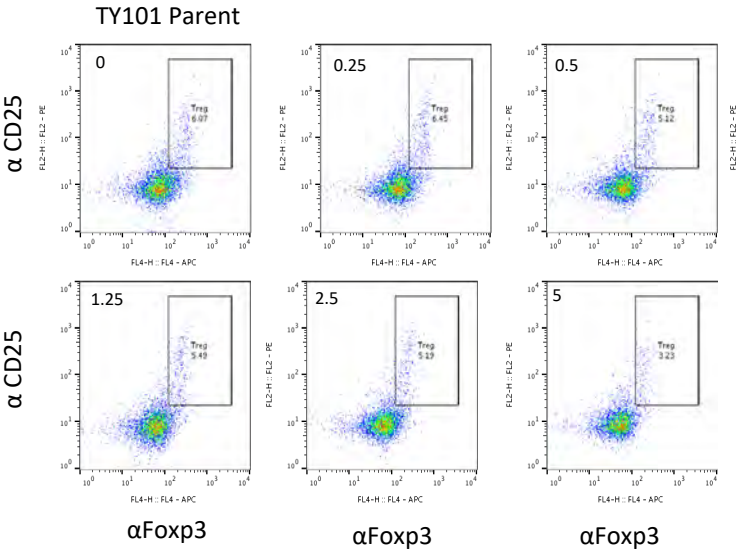

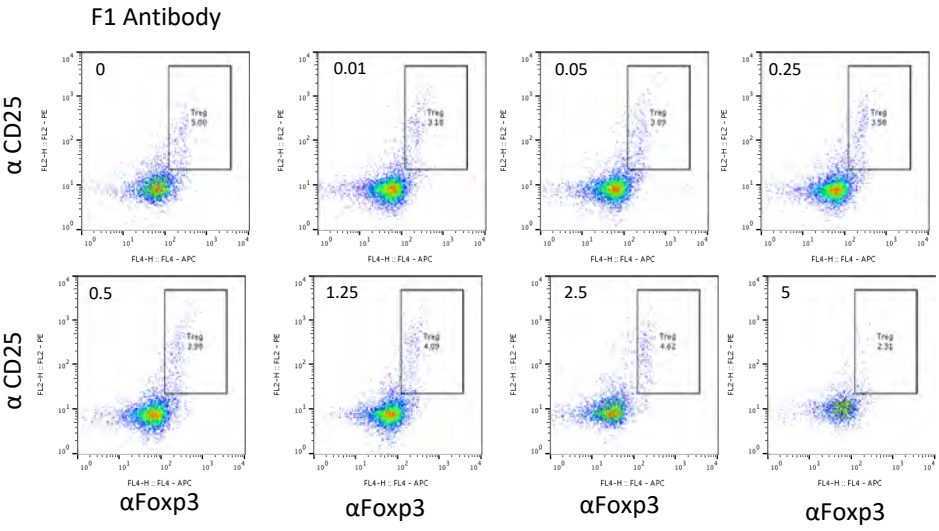

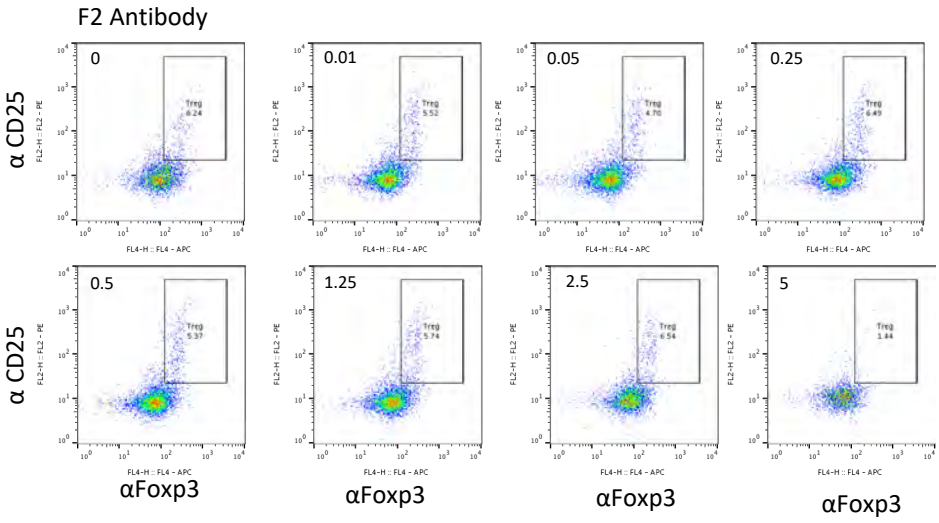

Day 8 Harvested Tumor Tissue

Supplementary Figure 4

PD1

TNFR2

Tregs

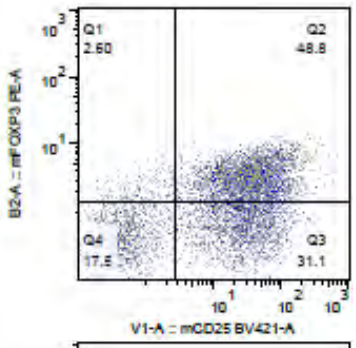

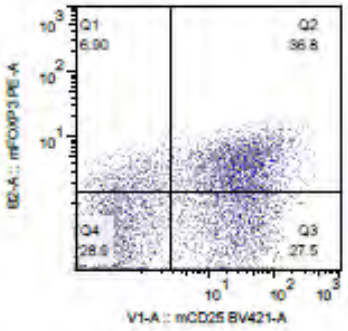

Teffs

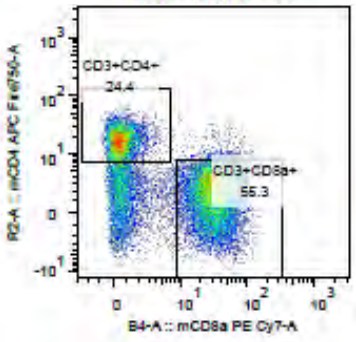

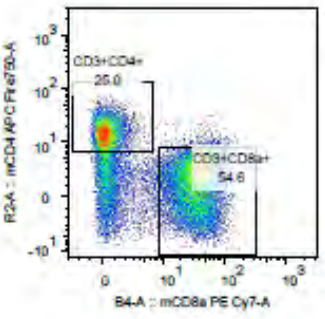

Supplementary Figure 5

Day 20 Harvested Tumor Tissue

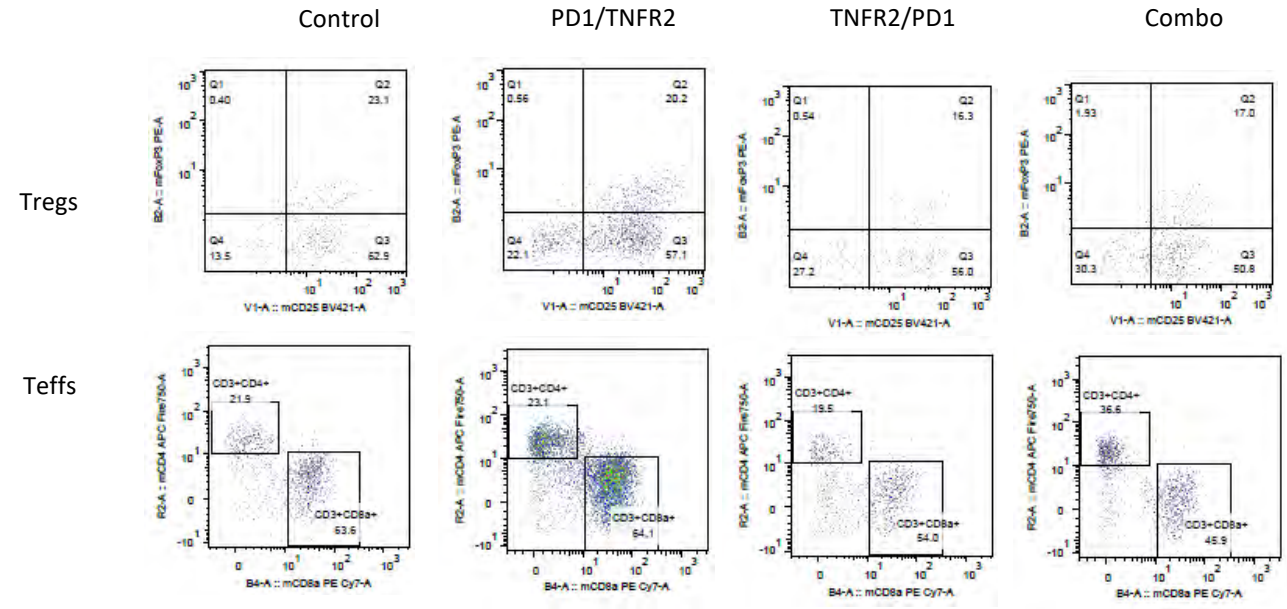

Supplementary Figure 6